

# Magnetic, Thermal, and Transport Properties of Layered Arsenides BaRu<sub>2</sub>As<sub>2</sub> and SrRu<sub>2</sub>As<sub>2</sub>

R. Nath, Yogesh Singh, and D. C. Johnston

Ames Laboratory and Department of Physics and Astronomy, Iowa State University, Ames, Iowa 50011, USA

(Dated: November 2, 2018)

The magnetic, thermal and transport properties of polycrystalline BaRu<sub>2</sub>As<sub>2</sub> and SrRu<sub>2</sub>As<sub>2</sub> samples with the ThCr<sub>2</sub>Si<sub>2</sub> structure were investigated by means of magnetic susceptibility  $\chi(T)$ , electrical resistivity  $\rho(T)$ , and heat capacity  $C_p(T)$  measurements. The temperature ( $T$ ) dependence of  $\rho$  indicates metallic character for both compounds with residual resistivity ratios  $\rho(310\text{ K})/\rho(2\text{ K})$  of 17 and 5 for the Ba and Sr compounds, respectively. The  $C_p(T)$  results reveal a low- $T$  Sommerfeld coefficient  $\gamma = 4.9(1)$  and  $4.1(1)$  mJ/mol K<sup>2</sup> and Debye temperature  $\Theta_D = 271(7)$  K and  $271(4)$  K for the Ba and Sr compounds, respectively. The  $\chi(T)$  was found to be diamagnetic with a small absolute value for both compounds. No transitions were found for BaRu<sub>2</sub>As<sub>2</sub> above 1.8 K. The  $\chi(T)$  data for SrRu<sub>2</sub>As<sub>2</sub> exhibit a cusp at  $\sim 200$  K, possibly an indication of a structural and/or magnetic transition. We discuss the properties of BaRu<sub>2</sub>As<sub>2</sub> and SrRu<sub>2</sub>As<sub>2</sub> in the context of other ThCr<sub>2</sub>Si<sub>2</sub>-type and ZrCuSiAs-type transition metal pnictides.

PACS numbers: 74.70.-b, 75.40.Cx, 65.40.Ba

## I. INTRODUCTION

The recent discovery of superconductivity in the layered oxypnictide compound LaFeAsO<sub>1-x</sub>F<sub>x</sub> with superconducting transition temperature  $T_c = 26$  K has generated great excitement.<sup>1</sup> Subsequently a series of compounds LnFeAsO<sub>1-x</sub>F<sub>x</sub> (e.g., Ln = Ce, Nd, and Sm) (abbreviated as 1111) have been reported with  $T_c$  ranging from 10 K to 55 K,<sup>2,3,4,5</sup> where the high  $T_c$  of 55 K was reached for SmFeAsO<sub>1-x</sub>F<sub>x</sub>.<sup>2</sup> All these compounds crystallize in a tetragonal unit cell of ZrCuSiAs structure type.<sup>6</sup> Later on another series of compounds A<sub>1-x</sub>K<sub>x</sub>Fe<sub>2</sub>As<sub>2</sub> (A = Ba, Sr, Ca, and Eu) (122) (Refs. 7,8,9,10,11) with the tetragonal ThCr<sub>2</sub>Si<sub>2</sub> structure type<sup>12</sup> was discovered where the maximum  $T_c$  achieved was 38 K.

A common feature of both 1111 and 122 compounds is the identical FeAs layers separated by the LnO or A layers perpendicular to the crystallographic  $c$ -axis. Undoped metallic parent compounds of both types show a spin-density wave (SDW) which coexists with a distorted structure at temperatures  $T \lesssim 200$  K.<sup>4,13,14,15,16,17,18,19,20</sup> Superconductivity in both series is sometimes assumed to be intimately connected with the SDW anomaly in the FeAs layers.<sup>7,13</sup> Electron or hole doping suppresses both the SDW and structural transition and facilitates the superconductivity. However, it is still unresolved whether the structural transition and/or the magnetism associated with the SDW play a vital role for the occurrence of superconductivity. There exist a few 122 compounds BaNi<sub>2</sub>P<sub>2</sub>,<sup>21</sup> BaNi<sub>2</sub>As<sub>2</sub>,<sup>22</sup> LaRu<sub>2</sub>P<sub>2</sub>,<sup>23</sup> CsFe<sub>2</sub>As<sub>2</sub>, and KFe<sub>2</sub>As<sub>2</sub>,<sup>10</sup> where even the undoped compound itself shows superconductivity at low temperatures. It is of interest to look for further new systems with different transition metal ions where one can try to achieve an enhanced  $T_c$ .

Motivated by the above progress, we turned our attention towards Ru-based layered compounds. So far in

the Ru series, LaRu<sub>2</sub>P<sub>2</sub> which has the ThCr<sub>2</sub>Si<sub>2</sub>-type structure is known to have  $T_c = 4.1$  K.<sup>23</sup> BaRu<sub>2</sub>As<sub>2</sub> and SrRu<sub>2</sub>As<sub>2</sub> compounds also crystallize in the body-centered tetragonal ThCr<sub>2</sub>Si<sub>2</sub> structure with space group  $I4/mmm$ . The reported lattice constants are ( $a = 4.152$  Å,  $c = 12.238$  Å) and ( $a = 4.168$  Å,  $c = 11.179$  Å) for the Ba and Sr compounds, respectively.<sup>23,24</sup> As shown in Fig. 1, Ru atoms in a square lattice are coordinated by As to form infinite RuAs layers and the layers are separated by Ba layers, similar to the AFe<sub>2</sub>As<sub>2</sub> compounds. Because BaRu<sub>2</sub>As<sub>2</sub> and SrRu<sub>2</sub>As<sub>2</sub> are isoelectronic to the above undoped AFe<sub>2</sub>As<sub>2</sub> compounds, a comparison of the properties of these two series of compounds is of great interest. A detailed investigation of the physical properties of the Ru compounds has not been reported yet. Herein we report a detailed characterization of polycrystalline BaRu<sub>2</sub>As<sub>2</sub> and SrRu<sub>2</sub>As<sub>2</sub> by means of magnetic susceptibility  $\chi(T)$ , electrical resistivity  $\rho(T)$ , and heat capacity  $C_p(T)$  measurements. We will discuss the properties of BaRu<sub>2</sub>As<sub>2</sub> and SrRu<sub>2</sub>As<sub>2</sub> in the context of other ThCr<sub>2</sub>Si<sub>2</sub>-type and ZrCuSiAs-type transition metal pnictides. From this comparison, it appears that a large Stoner enhancement of the conduction electron spin susceptibility is needed for high  $T_c$  in this class of materials.

## II. EXPERIMENTAL DETAILS

Polycrystalline samples of BaRu<sub>2</sub>As<sub>2</sub> and SrRu<sub>2</sub>As<sub>2</sub> were prepared by solid state reaction techniques using elemental Ba (99.999% pure), Sr (99.99% pure), Ru (99.9999% pure), and As (99.999% pure). The stoichiometric mixtures in an Al<sub>2</sub>O<sub>3</sub> crucible were sealed inside an evacuated quartz tube. At first, the elements were heated slowly up to 610 °C at a rate of 80 °C/hr, kept there for 10 hours and then heated up to 850 °C and kept there for 20 hours. The samples were then progressively fired at 950 °C and 1000 °C for 20 hours, each followed

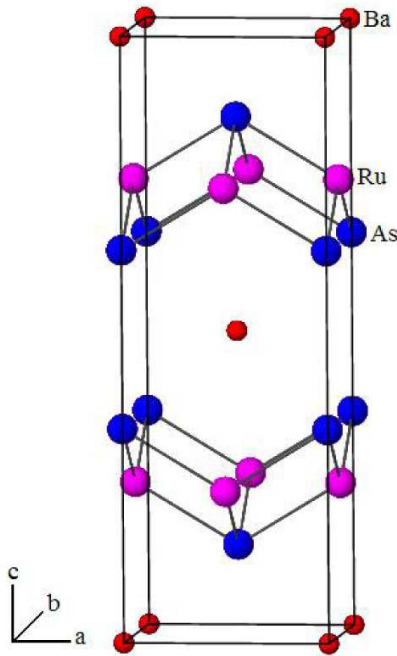


FIG. 1: (Color online) Crystal structure of  $\text{BaRu}_2\text{As}_2$  with the tetragonal  $\text{ThCr}_2\text{Si}_2$ -type structure showing RuAs layers and Ba layers alternating along the  $c$ -axis.

by one intermediate grinding and pelletization. For the final firing at  $1000^\circ\text{C}$ , the pellets were wrapped in a Ta foil before sealing in the quartz tube. All the sample handling was carried out inside a He-filled glove box. Our repeated attempts to grow crystals using Sn, Pb, and In fluxes followed by slow cooling failed.

The samples were characterized using a Rigaku Geigerflex powder X-ray diffractometer and  $\text{Cu K}\alpha$  radiation ( $\lambda_{av} = 1.54182 \text{ \AA}$ ). The powder pattern evidenced almost single phase material with a small impurity peak of about 2 and 3 percent relative intensity for the Ba and Sr compounds, respectively, which is suspected to arise from unreacted Ru. Unlike the Sr compound, for the Ba compound there appears another tiny impurity peak at the position expected for the strongest peak of  $\text{BaCO}_3$  at  $2\theta \approx 25^\circ$  (marked by a star) which has about 1.5% relative intensity. These impurities should not measurably affect the  $\chi(T)$  or  $C_p(T)$  data but may have an unknown effect on the  $\rho(T)$  data. Rietveld refinements of the data were carried out using the GSAS package.<sup>25</sup> Figure 2 shows the Rietveld refinement fit to the x-ray powder diffraction pattern for  $\text{BaRu}_2\text{As}_2$ . All the peaks except for the above impurity peak (see inset of Fig. 2) could be indexed and fitted based on the  $\text{ThCr}_2\text{Si}_2$  structure with  $I4/mmm$  space group. The goodness of the fit is 5.3% and 7.5% for the Ba and Sr compounds, respectively. The obtained lattice parameters are [ $a = 4.15248(8) \text{ \AA}$ ,  $c = 12.2504(3) \text{ \AA}$ ] and [ $a = 4.1713(1) \text{ \AA}$ ,  $c = 11.1845(4) \text{ \AA}$ ] for the Ba and Sr compounds, respectively. These values are close to the

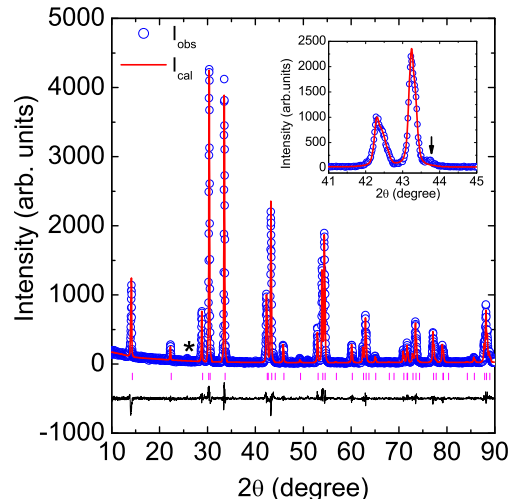


FIG. 2: (Color online) X-ray powder diffraction pattern (open circles) at room temperature for  $\text{BaRu}_2\text{As}_2$ . The solid line represents the Rietveld refinement fit with the  $\text{ThCr}_2\text{Si}_2$  structure and  $I4/mmm$  space group. The impurity peak corresponding to  $\text{BaCO}_3$  is marked by a star. Inset: small section of the x-ray powder pattern is magnified to highlight the unidentified impurity peak marked by an arrow, which might be due to unreacted Ru metal.

above previously reported ones.<sup>23</sup> Our refined  $z$  parameters for the As atoms are 0.3527(1) for  $\text{BaRu}_2\text{As}_2$  and 0.3612(2) for  $\text{SrRu}_2\text{As}_2$ .

The magnetization  $M$  and magnetic susceptibility  $\chi(T) \equiv M/H$ , where  $H$  is the applied magnetic field, were measured in the temperature  $T$  range  $1.8 \text{ K} \leq T \leq 300 \text{ K}$  on polycrystalline samples in a commercial Quantum Design SQUID (superconducting quantum interference device) magnetometer. DC resistivity  $\rho(T)$  was measured using a standard 4-probe technique by applying a current of 5 mA, and heat capacity  $C_p(T)$  was measured on a small piece of sample with mass about 8 mg. Both  $\rho(T)$  and  $C_p(T)$  measurements were performed on sintered pellets using a Quantum Design Physical Property Measurement System.

### III. EXPERIMENTAL RESULTS AND ANALYSIS

Figure 3 shows the temperature dependence of resistivity  $\rho(T)$  for  $\text{BaRu}_2\text{As}_2$  and  $\text{SrRu}_2\text{As}_2$ . With decreasing temperature,  $\rho(T)$  decreases for both compounds to a residual resistivity at 2 K of about  $9.7 \mu\Omega \text{ cm}$  and  $2300 \mu\Omega \text{ cm}$  for the Ba and Sr compounds, respectively. This type of temperature dependence suggests metallic behavior of the compounds. We did not observe any clear anomaly that might be associated with an SDW down to 2 K. The residual resistivity ratio  $\rho(310 \text{ K})/\rho(2 \text{ K})$  was

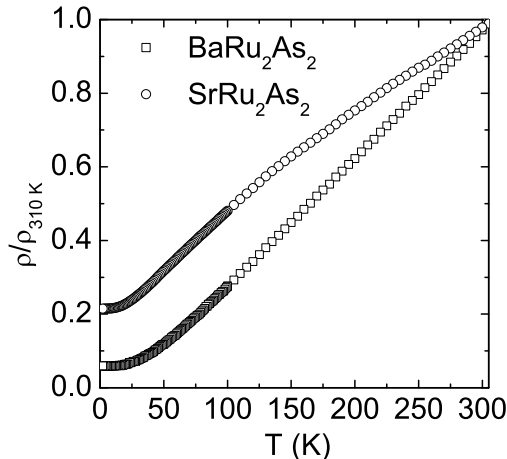


FIG. 3: Normalized DC electrical resistivity  $\rho$  versus temperature  $T$  of  $\text{BaRu}_2\text{As}_2$  and  $\text{SrRu}_2\text{As}_2$ . The room temperature resistivity  $\rho(310 \text{ K})$  values are  $170 \mu\Omega \text{ cm}$  and  $10.7 \text{ m}\Omega \text{ cm}$  for  $\text{BaRu}_2\text{As}_2$  and  $\text{SrRu}_2\text{As}_2$ , respectively. The unexpectedly large value for  $\text{SrRu}_2\text{As}_2$  may arise from a high porosity of the sample.

found to be about 17 and 5 for the Ba and Sr compounds, respectively. These values are comparable to those reported for polycrystalline  $(\text{Ba,Sr})\text{Fe}_2\text{As}_2$ .<sup>15,16</sup>

The heat capacity  $C_p$  vs.  $T$  at zero field for  $\text{BaRu}_2\text{As}_2$  and  $\text{SrRu}_2\text{As}_2$  is shown in Fig. 4. We did not observe any clear anomaly associated with a SDW or structural transition down to 2 K. However, the small anomaly at about 200 K for  $\text{SrRu}_2\text{As}_2$  may be a real effect in view of the cusp at the same temperature found in the measurement of  $\chi(T)$  below. The value of  $C_p$  at room temperature is about  $120 \text{ J/mol K}$  which is close to the Dulong Petit lattice heat capacity value  $C_p = 15R \simeq 125 \text{ J/mol K}$  expected for our compounds,<sup>26</sup> where  $R$  is the molar gas constant. As shown in the inset of Fig. 4,  $C_p(T)/T$  vs.  $T^2$  is almost linear at low- $T$  ( $T < 8 \text{ K}$ ) and was fitted by the expression  $C_p/T = \gamma + \beta T^2$ , where  $\gamma$  is the Sommerfeld coefficient of electronic heat capacity and the second term accounts for the lattice contribution with coefficient  $\beta$ . The resultant  $\gamma$  and  $\beta$  values are  $[4.9(1) \text{ mJ/mol K}^2$  and  $0.49(4) \text{ mJ/mol K}^4]$  and  $[4.1(1) \text{ mJ/mol K}^2$  and  $0.49(2) \text{ mJ/mol K}^4]$  for the Ba and Sr compounds, respectively.

The density of states at the Fermi energy for both spin directions  $N(E_F)$  can be estimated using the value of  $\gamma$  in the following relation,<sup>26</sup>

$$\gamma = \frac{\pi^2}{3} k_B^2 N(E_F) (1 + \lambda_{\text{ep}}) \quad (1)$$

where  $\lambda_{\text{ep}}$  is the electron-phonon coupling constant. As a first approximation we set  $\lambda_{\text{ep}} = 0$ , which gives  $N(E_F) = 2.1(1) \text{ states/(eV f.u.)}$  (f.u. stands for formula unit) and  $1.7(1) \text{ states/(eV f.u.)}$  for the Ba and Sr compounds, respectively. These densities of states are comparable with

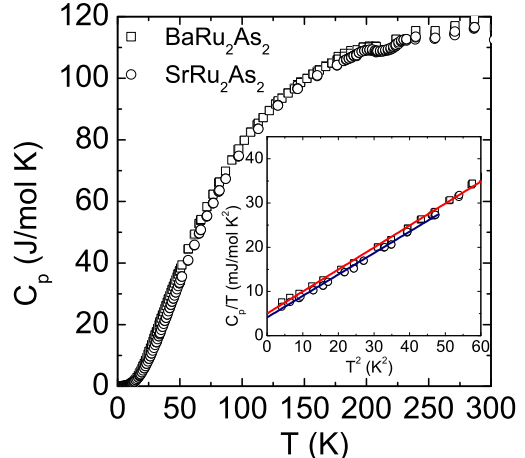


FIG. 4: (Color online) Heat capacity  $C_p$  vs. temperature  $T$  for  $\text{BaRu}_2\text{As}_2$  and  $\text{SrRu}_2\text{As}_2$ . The inset shows  $C_p/T$  vs.  $T^2$  at low temperatures and the two solid lines are the respective linear fits.

our previously reported value of  $2.0(4) \text{ states/(eV f.u.)}$  for  $\text{BaRh}_2\text{As}_2$  estimated in the same way from heat capacity measurements.<sup>27</sup> In  $\text{BaRh}_2\text{As}_2$ , band structure calculations indicate that the maximum contribution to  $N(E_F)$  comes from the Rh  $4d$  states.<sup>27</sup> From  $N(E_F)$  one can calculate the bare Pauli paramagnetic spin susceptibility of the conduction carriers  $\chi_P$  using<sup>26</sup>

$$\chi_P = \mu_B^2 N(E_F) \quad (2)$$

where  $\mu_B$  is the Bohr magneton. This gives  $\chi_P \simeq 6.8 \times 10^{-5} \text{ cm}^3/\text{mol}$  and  $5.5 \times 10^{-5} \text{ cm}^3/\text{mol}$  for the Ba and Sr compounds, respectively. These values are comparable to that found in  $\text{BaRh}_2\text{As}_2$ .<sup>27</sup> From the value of  $\beta$  one can also estimate the Debye temperature  $\Theta_D$  using the expression,<sup>26</sup>

$$\Theta_D = \left( \frac{12\pi^4 R n}{5\beta} \right)^{1/3} \quad (3)$$

where  $n$  is the number of atoms per formula unit ( $n = 5$  for our compounds). The above  $\beta$  values yield  $\Theta_D = 271(7) \text{ K}$  and  $271(4) \text{ K}$  for the Ba and Sr compounds, respectively, which are comparable to the values of  $\sim 280 \text{ K}$  (Ref. 28) and  $246(3) \text{ K}$  (Ref. 29) reported for isostructural  $\text{BaMn}_2\text{As}_2$  but are larger than the value of  $171(2) \text{ K}$  reported for  $\text{BaRh}_2\text{As}_2$ .<sup>27</sup>

For both the magnetic susceptibility  $\chi(T)$  and magnetization  $M(H, T)$  measurements we carried out, the data were corrected for the contribution of the empty sample holder, which was not negligible. The  $\chi \equiv M/H$  as a function of temperature in a field  $H = 1 \text{ T}$  is shown in Fig. 5, where the  $M$  data are corrected for the contributions from ferromagnetic impurities as determined from the  $M(H)$  isotherm data in Fig. 6 below.  $\chi(T)$  at high

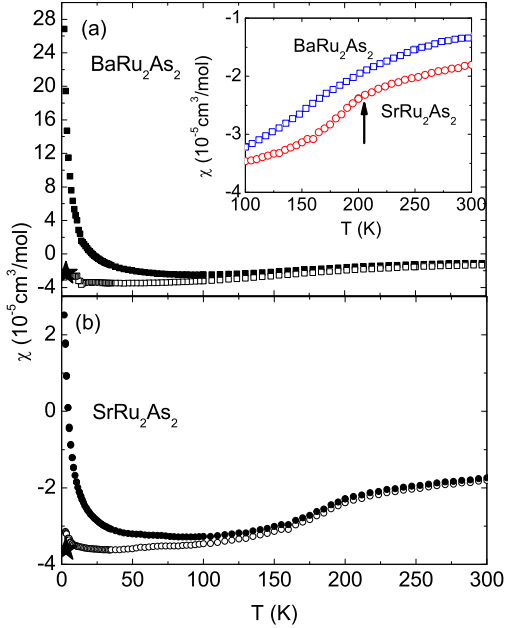


FIG. 5: (Color online) Magnetic susceptibility  $\chi \equiv M/H$  of (a)  $\text{BaRu}_2\text{As}_2$  and (b)  $\text{SrRu}_2\text{As}_2$  versus temperature  $T$  (solid symbols) measured in an applied magnetic field  $H = 1$  T. The magnetization  $M$  data are corrected for the contributions from ferromagnetic impurities as determined from the  $M(H)$  isotherm data in Fig. 6 (see text). The intrinsic  $\chi(T)$  after correction for the additional contribution of paramagnetic impurities (see text) is also shown (open symbols). The star symbols are the  $\chi_0$  values in Eq. (4) estimated from the analysis of magnetization versus field isotherms at low temperatures. In the inset of (a) the intrinsic  $\chi(T)$  data are magnified for both compounds and the arrow points to the anomaly around 200 K for  $\text{SrRu}_2\text{As}_2$ .

temperatures is negative and weakly temperature dependent. At low temperatures,  $\chi(T)$  shows a Curie-like upturn. For the Ba compound this upturn is much stronger than the Sr one. This upturn is attributed to extrinsic paramagnetic impurities and/or magnetic defects in the samples, as now discussed.

Magnetization  $M$  as a function of applied magnetic field  $H$  was measured at different temperatures. Figure 6 shows the  $M(H)$  isotherms at different temperatures for both compounds measured up to  $H = 5.5$  T. For both compounds  $M(H)$  shows a negative curvature below a field of 1 T at all temperatures due to the saturation of ferromagnetic impurities. To estimate the saturation magnetization  $M_s$  of the ferromagnetic impurities, we fitted magnetization isotherms at high temperatures [ $\geq 50$  K for  $\text{BaRu}_2\text{As}_2$  and  $\geq 25$  K for  $\text{SrRu}_2\text{As}_2$ ] to a straight line ( $M_s + \chi H$ ) above 1 T, as shown by the straight line fits in Fig. 6. The  $M_s$  was found to be nearly independent of  $T$  with values of about  $0.247$  G  $\text{cm}^3/\text{mol}$  and  $0.081$  G  $\text{cm}^3/\text{mol}$  at low temperatures for the Ba and

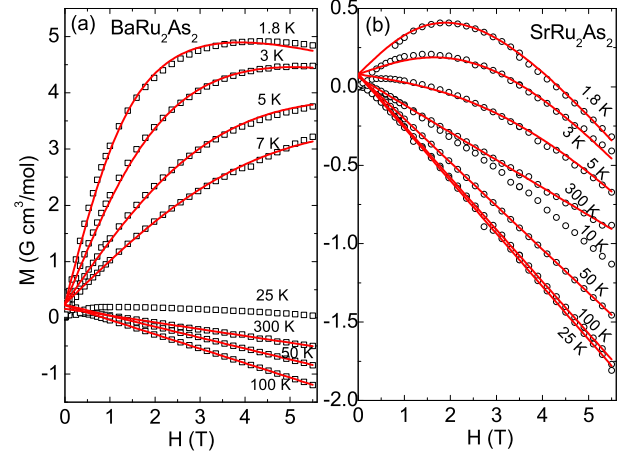


FIG. 6: (Color online) Magnetization  $M$  versus field  $H$  isotherms for (a)  $\text{BaRu}_2\text{As}_2$  and (b)  $\text{SrRu}_2\text{As}_2$  at different temperatures. For  $\text{SrRu}_2\text{As}_2$  at 1.8 K, we were not able to collect data below 5 kOe where the sum of the signals from the sample and sample holder is nearly zero. Solid curves are the fits by Eq. (4) at 1.8 K, 3 K, 5 K and 7 K for the Ba compound and at 1.8 K, 3 K and 5 K for the Sr compound. The straight lines are fits to the data for  $H \geq 1$  T at  $\geq 50$  K for the Ba compound and at  $\geq 25$  K for the Sr compound by  $M = M_s + \chi H$ .

Sr compounds, respectively. The near constant values of  $M_s$  versus temperature indicate that the Curie temperature(s) of the ferromagnetic impurities are significantly above 300 K. The low- $T$   $M_s$  values correspond to the contributions of the equivalent of 20 molar ppm and 6.6 molar ppm of Fe metal impurities to the  $M$  of the Ba and Sr compounds, respectively. The plotted magnetic susceptibilities at  $H = 1$  T as given above by the filled symbols in Fig. 5 are given by  $\chi(T) = [M(T) - M_s(T)]/H$ .

For a quantitative estimation of the paramagnetic impurity contribution giving rise to the upturns in the susceptibilities at low temperatures, we fitted our  $M(H)$  data for  $1 \text{ T} \leq H \leq 5.5 \text{ T}$  at 1.8 K, 3 K, 5 K and 7 K for the Ba compound and 1.8 K, 3 K and 5 K for the Sr compound simultaneously by the equation

$$M = M_s + \chi_0 H + f_{\text{imp}} N_A g_{\text{imp}} \mu_B S_{\text{imp}} B_{S_{\text{imp}}}(x) \quad (4)$$

where  $M_s$  is the above-determined low-temperature ferromagnetic impurity saturation value,  $f_{\text{imp}}$  is the molar fraction of the impurities,  $N_A$  is Avogadro's number,  $g_{\text{imp}}$  is the impurity  $g$ -factor,  $S_{\text{imp}}$  is the impurity spin,  $B_{S_{\text{imp}}}(x)$  is the Brillouin function,<sup>26</sup> and  $\chi_0$  is the intrinsic susceptibility of the sample. The modified argument of the Brillouin function is  $x = g_{\text{imp}} \mu_B S_{\text{imp}} H / [k_B (T - \theta_{\text{imp}})]$  where  $\theta_{\text{imp}}$  is the Weiss temperature due to impurity interactions. To reduce the number of fitting parameters, the impurity  $g$ -factor was set to  $g_{\text{imp}} = 2$ . The obtained fitting parameters ( $\chi_0$ ,  $f_{\text{imp}}$ ,  $S_{\text{imp}}$ , and

$\theta_{\text{imp}}$ ) are  $[-2.3(1) \times 10^{-5} \text{ cm}^3/\text{mol}$ ,  $0.0284(3) \text{ mol}\%$ ,  $1.85(3)$ , and  $-0.46(6) \text{ K}$ ] and  $[-3.62(6) \times 10^{-5} \text{ cm}^3/\text{mol}$ ,  $0.0092(1) \text{ mol}\%$ ,  $1.62(4)$ , and  $-1.2(1) \text{ K}$ ] for the Ba and Sr compounds, respectively. The Curie constant  $C_{\text{imp}}$  of the paramagnetic impurities was calculated using  $C_{\text{imp}} = f_{\text{imp}} N_A g_{\text{imp}}^2 \mu_B^2 S_{\text{imp}}(S_{\text{imp}} + 1)/3k_B$  which yields  $C_{\text{imp}} \approx 0.754 \times 10^{-3} \text{ cm}^3 \text{ K/mol}$  and  $0.195 \times 10^{-3} \text{ cm}^3 \text{ K/mol}$  for the Ba and Sr compounds, respectively. Our intrinsic  $\chi(T)$  data that are corrected for both the ferromagnetic impurity and paramagnetic impurity contributions are shown in Fig. 5 as open symbols. The low- $T$   $\chi_0$  values obtained from the magnetization isotherm analysis are also plotted as filled stars in Fig. 5 and are, of course, in agreement with the intrinsic  $\chi(T)$  data.

From the open symbols in Fig. 5, the intrinsic susceptibilities of  $\text{BaRu}_2\text{As}_2$  and  $\text{SrRu}_2\text{As}_2$  are diamagnetic over the whole  $T$  range, becoming somewhat more negative with decreasing  $T$ . A diamagnetic susceptibility is not unprecedented for a transition metal compound, as seen, e.g., for  $\text{LaRu}_2\text{P}_2$  [Ref. 23] and  $\text{OsB}_2$  and  $\text{RuB}_2$ .<sup>30</sup> As shown in the inset of Fig. 5, the intrinsic  $\chi(T)$  of  $\text{SrRu}_2\text{As}_2$  shows a (reproducible) small cusp around 200 K in contrast to the smooth behavior observed in  $\text{BaRu}_2\text{As}_2$ . This cusp for  $\text{SrRu}_2\text{As}_2$  is qualitatively similar to the cusp seen for 1111 and 122 parent compounds and attributed to structural/SDW transitions.<sup>4,13,14,15,16,17,18,19,20</sup> The temperature of the cusp is similar to the temperature of the small anomaly in  $C_p(T)$  in Fig. 4, so the latter anomaly may not be an artifact.

#### IV. DISCUSSION

The intrinsic  $\chi(T)$  of a metal can be written as  $\chi = \chi_D + \chi_{VV} + \chi_P$ , where  $\chi_D$  includes the orbital diamagnetism of the core electrons ( $\chi_{\text{core}}$ ) and the orbital Landau diamagnetism ( $\chi_L$ ) of the conduction electrons,  $\chi_{VV}$  is the orbital Van Vleck paramagnetism, and  $\chi_P$  is the Pauli spin paramagnetism of the conduction electrons. For an extended system it is difficult to calculate  $\chi_D$  due to intercell currents. Nevertheless one can roughly estimate the  $\chi_{\text{core}}$  of the compounds assuming an ionic picture, where (Ba or Sr), Ru, and As are in 2+, 2+, and 3- oxidation states, respectively.<sup>31</sup> This estimate will give the upper limit to the  $\chi_D$ . In this way  $\chi_{\text{core}}$  was calculated to be  $-1.6 \times 10^{-4} \text{ cm}^3/\text{mol}$  and  $-1.43 \times 10^{-4} \text{ cm}^3/\text{mol}$  for the Ba and Sr compounds, respectively. Since  $\chi_P$  is positive, when added to the negative  $\chi_{\text{core}}$ , the result is a reduced positive value or even a negative value of  $\chi$ . Using the  $\chi_P$  values obtained from the above heat capacity data analysis, the sum of  $\chi_{\text{core}}$  and  $\chi_P$  is  $\approx -9 \times 10^{-5} \text{ cm}^3/\text{mol}$  for both compounds. This value is somewhat more negative than the intrinsic values in Fig. 5, suggesting that the Van Vleck paramagnetic orbital susceptibility  $\chi_{VV}$  and/or Stoner enhancement of  $\chi_P$  are not negligible in these compounds. This value is also of the same order of magnitude as has been estimated

for  $\text{BaRh}_2\text{As}_2$ .<sup>27</sup>

In the following discussion we relate the properties of the (Sr,Ba) $\text{Ru}_2\text{As}_2$  compounds with those of other  $\text{ThCr}_2\text{Si}_2$ -type and  $\text{ZrCuSiAs}$ -type pnictides and consider their superconducting transition temperature  $T_c$  or lack thereof. Lee and coworkers<sup>32,33</sup> and Zhao and coworkers<sup>34</sup> found an interesting correlation for a wide range of parent compounds  $\text{Ba}(\text{Fe,Ni})_2(\text{P,As})_2$  and  $\text{Ln}(\text{Fe,Ni})(\text{P,As})\text{O}$  where  $\text{Ln}$  is a rare earth element: the highest  $T_c$  occurred for the doped materials in which the respective  $\text{FeAs}_4$  tetrahedra were least distorted.<sup>32,33,34</sup> Within a  $\text{MPn}_4$  tetrahedron where  $M$  is the transition metal and  $\text{Pn} = \text{P}$  or  $\text{As}$ , there is a two-fold  $\text{Pn-M-Pn}$  bond angle where the two  $\text{Pn}$  atoms are on the same side of the  $M$  atom layer along the  $c$  axis, and there is a four-fold  $\text{Pn-M-Pn}$  bond angle where the two  $\text{Pn}$  atoms are on opposite sides of the  $M$  layer (see Fig. 1). The angle plotted in Refs. 32 and 33 is the two-fold  $\text{Pn-M-Pn}$  bond angle.

We have calculated the two-fold As-Ru-As bond angles from our structural data for the (Sr,Ba) $\text{Ru}_2\text{As}_2$  compounds and also for the As-Rh-As bond angle for  $\text{BaRh}_2\text{As}_2$ .<sup>27</sup> For the body-centered-tetragonal  $\text{BaFe}_2\text{As}_2$ -type and the primitive tetragonal  $\text{LaFeAsO}$ -type structures, the two-fold and four-fold As-Fe-As bond angles are given by

$$\begin{aligned} \theta_2 &= \arccos \left[ \frac{-\frac{a^2}{4} + (z - \alpha)^2 c^2}{r^2} \right] & (2\text{-fold}) \\ \theta_4 &= \arccos \left[ \frac{-(z - \alpha)^2 c^2}{r^2} \right] & (4\text{-fold}) \end{aligned}$$

where

$$r^2 = \frac{a^2}{4} + (z - \alpha)^2 c^2 \quad (5)$$

and  $\alpha = 1/4$  for the  $\text{BaFe}_2\text{As}_2$ -type structure and  $\alpha = 1/2$  for the  $\text{LaFeAsO}$ -type structure. Here  $a$  and  $c$  are the lattice parameters,  $z$  is the  $z$ -axis position parameter of the As atom in the respective structure ( $z \approx 0.35$  in  $\text{BaFe}_2\text{As}_2$  and  $z \approx 0.65$  in  $\text{LaFeAsO}$ ), and  $r$  is the nearest-neighbor Fe-As distance within an Fe-centered  $\text{FeAs}_4$  tetrahedron (all four Fe-As nearest-neighbor distances are the same in each of the two structures). The Fe atoms in both structures form a square lattice where the 4-fold nearest-neighbor Fe-Fe distance in both structures is  $d_{\text{Fe-Fe}} = a/\sqrt{2}$ .

Using Eqs. (5), we find  $\theta_2 = 117.6^\circ$ ,  $118.4^\circ$ , and  $112.2^\circ$  for  $\text{BaRu}_2\text{As}_2$ ,  $\text{SrRu}_2\text{As}_2$  and  $\text{BaRh}_2\text{As}_2$ , respectively. These bond angles for the (Ba,Sr) $\text{Ru}_2\text{As}_2$  compounds are significantly larger than the above optimum value of  $\approx 110^\circ$  for the Fe(P,As)-based materials and therefore the low  $T_c$ 's  $< 1.8 \text{ K}$  for the (Ba,Sr) $\text{Ru}_2\text{As}_2$  compounds are consistent with this overall behavior. On the other hand,  $\text{BaRh}_2\text{As}_2$  stands out as an exception: it has the same  $\theta_2$  as the high temperature superconducting  $\text{LaFeAsO}$ -based and  $\text{CeFeAsO}$ -based compounds with  $T_c = 28\text{--}40 \text{ K}$  (Refs. 32 and 34) but is not superconducting. Therefore, at least one additional characteristic

of the materials must be controlling  $T_c$ . As will be discussed in detail elsewhere,<sup>35</sup> the bare nonmagnetic band structure density of states at the Fermi energy  $N(E_F)$  is not correlated with  $T_c$ . For example, the calculated  $N(E_F)$  for nonsuperconducting  $\text{BaRh}_2\text{As}_2$  and that of superconducting  $\text{LaFeAsO}_{0.9}\text{F}_{0.1}$  with  $T_c = 27$  K are the same. The values are 1.76 [Ref. 27] and 1.28–2.01 states/(eV- $M$  atom) [Refs. 36 and 37], respectively, for both spin directions.

On the other hand,  $\chi(300$  K) is large for all FeAs-based compounds with high  $T_c$ , suggesting that Stoner enhancement of the susceptibility may be relevant to the superconducting mechanism.<sup>35</sup> Again using the same examples as above, for  $\text{BaRh}_2\text{As}_2$  one finds a powder averaged  $\bar{\chi}(300$  K) =  $0.18 \times 10^{-4}$  cm<sup>3</sup>/(mol Rh),<sup>27</sup> whereas for  $\text{LaFeAsO}_{0.9}\text{F}_{0.1}$  one obtains  $\bar{\chi}(300$  K) =  $3.3 \times 10^{-4}$  cm<sup>3</sup>/(mol Fe),<sup>38</sup> which is a factor of 18 larger. For  $\text{LaFeAsO}_{0.9}\text{F}_{0.1}$ , the above  $N(E_F)$  range predicts a bare Pauli conduction electron spin susceptibility of 0.41– $0.65 \times 10^{-4}$  cm<sup>3</sup>/(mol Fe), suggesting a Stoner enhancement by a factor of 5 to 8. However, accurate estimates of the enhancement factor require that orbital contributions to  $\chi$  must be corrected for.<sup>35</sup>

## V. CONCLUSION

We have synthesized and investigated the physical properties of  $\text{ThCr}_2\text{Si}_2$ -type polycrystalline  $\text{BaRu}_2\text{As}_2$  and  $\text{SrRu}_2\text{As}_2$  compounds. Both compounds were found to be metallic in character. Unlike other similar *isoelectronic* compounds  $(\text{Ca,Sr,Ba})\text{Fe}_2\text{As}_2$ ,  $\text{BaRu}_2\text{As}_2$  shows no signature of a spin density wave or a structural transition from  $\rho(T)$ ,  $\chi(T)$  or  $C_p(T)$  measurements down to

1.8 K. However, a clear cusp in  $\chi(T)$  and a hint of one in  $C_p(T)$  was found at  $\sim 200$  K for  $\text{SrRu}_2\text{As}_2$ , which may be indicative of a structural and/or magnetic transition.

From analysis of our  $C_p(T)$  data, the density of states at the Fermi energy  $N(E_F)$  for  $(\text{Ba,Sr})\text{Ru}_2\text{As}_2$  was estimated to be  $\sim 1$  state/(eV Ru atom) for both spin directions and is comparable to that per Rh atom in  $\text{BaRh}_2\text{As}_2$ . The small and negative values of  $\chi(T)$  for both  $\text{BaRu}_2\text{As}_2$  and  $\text{SrRu}_2\text{As}_2$  indicate small or negligible Stoner enhancement of the conduction electron spin susceptibility. A comparison of  $N(E_F)$  with that of  $\text{BaRh}_2\text{As}_2$  suggests that the maximum contribution to  $N(E_F)$  comes from the Ru 4d states. It would be interesting to study the effect of doping of  $\text{SrRu}_2\text{As}_2$  in view of the occurrence of superconductivity in  $\text{Ba}_{1-x}\text{K}_x\text{Fe}_2\text{As}_2$ ,  $\text{Sr}_{1-x}\text{K}_x\text{Fe}_2\text{As}_2$  and  $\text{BaFe}_{2-x}\text{Ru}_x\text{As}_2$ .<sup>7,10,39</sup> Finally, a comparison of the properties of  $(\text{Ba,Sr})\text{Ru}_2\text{As}_2$  and  $\text{BaRh}_2\text{As}_2$  with those of the FeAs-based materials indicates that  $N(E_F)$  for these nonsuperconducting Ru and Rh arsenides is about the same as for FeAs-based compounds with high  $T_c$ .<sup>35</sup> A distinguishing feature of the high  $T_c$  FeAs-based materials is their large  $\chi$  values that evidently reflect significant Stoner enhancement of the conduction electron spin susceptibility<sup>35</sup> as has been pointed out before.<sup>40,41,42</sup> Thus it seems possible that the mechanisms for the Stoner enhancement and for the high  $T_c$  in the FeAs-based materials may be closely related.

## Acknowledgments

Work at the Ames Laboratory was supported by the Department of Energy-Basic Energy Sciences under Contract No. DE-AC02-07CH11358.

- 
- <sup>1</sup> Y. Kamihara, T. Watanabe, M. Hirano, and H. Hosono, *J. Am. Chem. Soc.* **130**, 3296 (2008).
- <sup>2</sup> Z.-A. Ren, L. Wei, Y. Jie, Y. Wei, S. X. Li, Z. Cai, C. G. Can, D. X. Li, S. L. Ling, Z. Fang, and Z. Z. Xian, *Chin. Phys. Lett.* **25**, 2215 (2008).
- <sup>3</sup> X. H. Chen, T. Wu, G. Wu, R. H. Liu, H. Chen, and D. F. Fang, *Nature* **453**, 761 (2008).
- <sup>4</sup> G. F. Chen, Z. Li, D. Wu, G. Li, W. Z. Hu, J. Dong, P. Zheng, J. L. Luo, and N. L. Wang, *Phys. Rev. Lett.* **100**, 247002 (2008).
- <sup>5</sup> Z.-A. Ren, J. Yang, W. Lu, W. Yi, X.-L. Shen, Z.-C. Li, G.-C. Che, X.-L. Dong, L.-L. Sun, F. Zhou, and Z.-X. Zhao, *Europhys. Lett.* **82**, 57002 (2008).
- <sup>6</sup> P. Quebe, L. Terbuchte, and W. Jeitschko, *J. Alloys Compd.* **302**, 70 (2000).
- <sup>7</sup> M. Rotter, M. Tegel, and D. Johrendt, *Phys. Rev. Lett.* **101**, 107006 (2008).
- <sup>8</sup> G. F. Chen, Z. Li, G. Li, W.-Z. Hu, J. Dong, J. Zhou, X.-D. Zhang, P. Zheng, N.-L. Wang, and J.-L. Luo, *Chin. Phys. Lett.* **25**, 3403 (2008).
- <sup>9</sup> H. S. Jeevan, Z. Hossain, D. Kasinathan, H. Rosner, C. Geibel, and P. Gegenwart, *Phys. Rev. B* **78**, 092406 (2008).
- <sup>10</sup> K. Sasmal, B. Lv, B. Lorenz, A. M. Guloy, F. Chen, Y.-Y. Xue, and C. W. Chu, *Phys. Rev. Lett.* **101**, 107007 (2008).
- <sup>11</sup> G. Wu, H. Chen, Y. L. Xie, Y. J. Yan, R. H. Liu, X. F. Wang, J. J. Ying, and X. H. Chen, *J. Phys.: Condens. Matter* **20**, 422201 (2008).
- <sup>12</sup> M. Pfisterer and G. Nagorsen, *Z. Naturforsch. B* **35**, 703 (1980).
- <sup>13</sup> J. Dong, H. J. Zhang, G. Xu, Z. Li, G. Li, W. Z. Hu, D. Wu, G. F. Chen, X. Dai, J. L. Luo, Z. Fang, and N. L. Wang, *Europhys. Lett.* **83**, 27006 (2008).
- <sup>14</sup> H.-H. Klauss, H. Luetkens, R. Klingeler, C. Hess, F. J. Litterst, M. Kraken, M. M. Korshunov, I. Eremin, S.-L. Drechsler, R. Khasanov, A. Amato, J. Hamann-Borrero, N. Leps, A. Kondrat, G. Behr, J. Werner, and B. Büchner, *Phys. Rev. Lett.* **101**, 077005 (2008).
- <sup>15</sup> M. Rotter, M. Tegel, D. Johrendt, I. Schellenberg, W. Hermes, and R. Pöttgen, *Phys. Rev. B* **78**, 020503(R) (2008).
- <sup>16</sup> C. Krellner, N. Caroca-Canales, A. Jesche, H. Rosner, A. Ormeci and C. Geibel, *Phys. Rev. B* **78**, 100504(R) (2008).
- <sup>17</sup> N. Ni, S. L. Bud'ko, A. Kreyssig, S. Nandi, G. E. Rustan, A. I. Goldman, S. Gupta, J. D. Corbett, A. Kracher, and P. C. Canfield, *Phys. Rev. B* **78**, 014507 (2008).

- <sup>18</sup> J.-Q. Yan, A. Kreyssig, S. Nandi, N. Ni, S. L. Budko, A. Kracher, R. J. McQueeney, R. W. McCallum, T. A. Lograsso, A. I. Goldman, and P. C. Canfield, *Phys. Rev. B* **78**, 024516 (2008).
- <sup>19</sup> Z. Ren, Z. Zhu, S. Jiang, X. Xu, Q. Tao, C. Wang, C. Feng, G. Cao, and Z. Xu, *Phys. Rev. B* **78**, 052501 (2008).
- <sup>20</sup> H. S. Jeevan, Z. Hossain, D. Kasinathan, H. Rosner, C. Geibel, and P. Gegenwart, *Phys. Rev. B* **78**, 052502 (2008).
- <sup>21</sup> T. Mine, H. Yanagi, T. Kamiya, Y. Kamihara, M. Hirano, and H. Hosono, *Solid State Commun.* **147**, 111 (2008).
- <sup>22</sup> F. Ronning, N. Kurita, E. D. Bauer, B. L. Scott, T. Park, T. Klimczuk, R. Movshovich, and J. D. Thompson, *J. Phys.: Condens. Matter* **20**, 342203 (2008).
- <sup>23</sup> W. Jeitschko, R. Glaum, and L. Boonk, *J. Solid State Chem.* **69**, 93 (1987).
- <sup>24</sup> G. Wenski and A. Mewis, *Z. Naturforsch. B* **41**, 38 (1986).
- <sup>25</sup> A. C. Larson and R. B. Von Dreele, “General Structure Analysis System (GSAS)”, Los Alamos National Laboratory Report LAUR 86-748 (2000); B. H. Toby, *J. Appl. Cryst.* **34**, 210 (2001).
- <sup>26</sup> C. Kittel, *Introduction to Solid State Physics*, 4th ed. (Wiley, New York, 1966).
- <sup>27</sup> Y. Singh, Y. Lee, S. Nandi, A. Kreyssig, A. Ellern, S. Das, R. Nath, B. N. Harmon, A. I. Goldman, and D. C. Johnston, *Phys. Rev. B* **78**, 104512 (2008).
- <sup>28</sup> J. An, A. S. Sefat, D. J. Singh, M. H. Du, and D. Mandrus, arXiv:0901.0272 (2009).
- <sup>29</sup> Y. Singh, A. Ellern, and D. C. Johnston, arXiv:0901.3370 (2009).
- <sup>30</sup> Y. Singh, A. Niazi, M. D. Vannette, R. Prozorov, and D. C. Johnston, *Phys. Rev. B* **76**, 214510 (2007).
- <sup>31</sup> P. W. Selwood, *Magnetochemistry*, 2nd ed. (Interscience, New York, 1956), p. 78.
- <sup>32</sup> C.-H. Lee, A. Iyo, H. Eisaki, H. Kito, M. T. Fernandez-Diaz, T. Ito, K. Kihou, H. Matsuhata, M. Braden, and K. Yamada, *J. Phys. Soc. Jpn.* **77**, Suppl. C, 44 (2008).
- <sup>33</sup> C.-H. Lee, A. Iyo, H. Eisaki, H. Kito, M. T. Fernandez-Diaz, R. Kumai, K. Miyazawa, K. Kihou, H. Matsuhata, M. Braden, and K. Yamada, *J. Phys. Soc. Jpn.* **77**, 083704 (2008).
- <sup>34</sup> J. Zhao, Q. Huang, C. de la Cruz, S. Li, J. W. Lynn, Y. Chen, M. A. Green, G. F. Chen, G. Li, Z. Li, J. L. Luo, N. L. Wang, and P. Dai, *Nature Mater.* **7**, 953 (2008).
- <sup>35</sup> D. C. Johnston et al., (unpublished).
- <sup>36</sup> I. I. Mazin, D. J. Singh, M. D. Johannes, and M. H. Du, *Phys. Rev. Lett.* **101**, 057003 (2008).
- <sup>37</sup> G. Wang, Y. Qian, G. Xu, X. Dai, and Z. Fang, arXiv:0903.1385.
- <sup>38</sup> R. Klingeler, N. Leps, I. Hellmann, A. Popa, C. Hess, A. Kondrat, J. Hamann-Borrero, G. Behr, V. Kataev, and B. Büchner, arXiv:0808.0708; A. Kondrat, J. E. Hamann-Borrero, N. Leps, M. Kosmala, O. Schumann, J. Werner, G. Behr, M. Braden, R. Klingeler, B. Büchner, and C. Hess, arXiv:0811.4436; R. Klingeler, private communication.
- <sup>39</sup> S. Paulraj, S. Sharma, A. Bharathi, A. T. Satya, S. Chandra, Y. Hariharan, and C. S. Sundar, arXiv:0902.2728.
- <sup>40</sup> D. J. Singh and M.-H. Du, *Phys. Rev. Lett.* **100**, 237003 (2008); D. J. Singh, arXiv:0901.2149.
- <sup>41</sup> Y. Kohama, Y. Kamihara, M. Hirano, H. Kawaji, T. Atake, and H. Hosono, *Phys. Rev. B* **78**, 020512(R) (2008).
- <sup>42</sup> K. Haule and G. Kotliar, *New J. Phys.* **11**, 025021 (2009).